Electronic Supplementary Information (ESI)

Spontaneous resolution of a Δ/Λ-chiral-at-metal pseudo-tetrahedral Schiff-base Zinc complex to a racemic conglomerate with C–H···O organized 4_1- and 4_3-helices

Mohammed Enamullah,[a,*] Vera Vasylyeva,[b] Mohammad Abdul Quddus,[a] Mohammad Khairul Islam,[a] Simon-Patrick Höfert[b] and Christoph Janiak[b,*]

[a] Department of Chemistry, Jahangirnagar University, Dhaka-1342, Bangladesh. E-mail: enamullah@juniv.edu

[b] Institut für Anorganische Chemie und Strukturchemie, Heinrich-Heine-Universität, Universitätsstr. 1, D-40225 Düsseldorf, Germany. Email: janiak@uni-duesseldorf.de

Additional Emails: enamullah@juniv.edu, Vira.Vasylyeva@ruhr-uni-bochum.de, md.abdulquddus@rocketmail.com, khairul_chemist@outlook.com, Hoefert@hhu.de, janiak@hhu.de

Case studies of spontaneous resolution in Zn(II)-pseudo-tetrahedral complexes with achiral ligands showing supramolecular *P* (right)- and *M* (left)-helices:

Spontaneous resolution in Zn(II)-complexes to provide double helical motifs in $[Zn(L)Cl_2]$ and $[Zn(L)Br_2]$ {L = 2,6-bis(imidazol-1-yl)pyridine} with both right (*P*)- and left (*M*)-helicity in each.[1] Two Cl (or Br) atoms on each $ZnCl_2$ (or $ZnBr_2$) unit are involved in hydrogen bonding interactions with the imidazole- and pyridyl-H atoms and O-atoms of guest H_2O molecules, interlocking the double helices laterally into a densely packed homochiral 3D-coordination framework.

Hydrothermal reactions of flexible multi-carboxylate bridged ligand (H_4ODPA = 2,2',3,3'-oxydiphthalic acid) with Zn or Cd(II)-salt in presence of 4,4'-bipyridine (bpy) afford two homochiral right (*P*)-handed helical coordination polymers in each via spontaneous resolution. They have different chiral space groups $P2_12_12_1$ for Zn(II) or $P2_1$ for Cd(II) and different bridging modes of the 2,2',3,3'-ODPA ligand.[2] The same reaction with Cu or Ni(II)-salts provide a homochiral left (*M*)-handed or right (*P*)-handed helix with space groups $P3_121$ or $C2$.

Spontaneous resolution with *P*- and *M*-helicity in enantiomeric pair $[M(L)(SO_4)(H_2O)]_n$ (M = Zn or Co; L =1,4-bis(4-pyridyl)-2,3-diaza-1,3-butadiene)[3] have been synthesized as a racemic conglomerate of 2D metal organic frameworks (MOFs) by O−H···O hydrogen bonding interactions. In presence of enantiopure camphoric acid, crystallization process prefers absolute chiral induction over conglomerate formation.

Two homochiral compounds $[Zn(S \text{ or } R)\text{-tzt})]_n$ and $[Zn(S \text{ or } R)\text{-tzp})(H_2O)_2]\cdot H_2O$ (H_2tzt/H_2tzp = *N*-[2-(1*H*-tetrazol-5-yl)ethyl]-tryptophan/proline) have reported, in which the former compounds feature a 2D framework generated by N–H···π interactions between two adjacent indole rings, with chiral space group $P2_12_12_1$. While the later one is stabilized by extensive hydrogen bonds, leads to the formation of a supramolecular 2D architecture.[4]

The compound $Zn(OHPTs)(H_2O)$ (H_2OHPTs = *N*,*N*′-bis(2-tosylaminobenzylidene)-1,3-diamino-2-propanol) crystallizes with spontaneous resolution to provide enantiopure Λ-helices. The crystal packing is due to hydrogen bonding network among OH-spacer groups, water molecules and O atoms of tosyl groups, forms channels along the crystal.[5]

Using achiral ligand α,α'-*bis*(pyrazolyl)-*m*-xylene (L), a 1-D coordination polymer $[Zn(L)Cl_2]_\alpha$ as conglomerate with left (*M*)- and right (*P*)-handed homochiral helices were isolated via spontaneous resolution. Helical channels are formed by the lock of flexible bridging ligand (L) in a twisted chiral environment and noncovalent C–H···Cl hydrogen-bonding supported by π···π interactions.[6]

Achiral 2,5-diphenyl-3,4-di(3-pyridyl)cyclopenta-2,4-dien-1-one (L) coordinates to the $ZnCl_2$ or $HgBr_2$, and affords the helically chiral coordination polymers $[(L)ZnCl_2]_\alpha$ or $[(L)HgBr_2]_\alpha$ via spontaneous resolution, forming colonies of homochiral (*M*-helix) single crystals.[7a] The neighbouring chains are united by π···π interactions between phenyl groups and cyclopentadienone units.

The hexafluorophosphate salts of metal(II) cations with 2,2'-bipyridine provide racemic compounds for Fe(II) and Ru(II) ions, or conglomerates for Zn(II) ion.[7b] In the racemic compounds (C–H···π) interactions are present between the coordinated ligands, while in the conglomerates π–π stacking dominates.

[1]H NMR spectra.

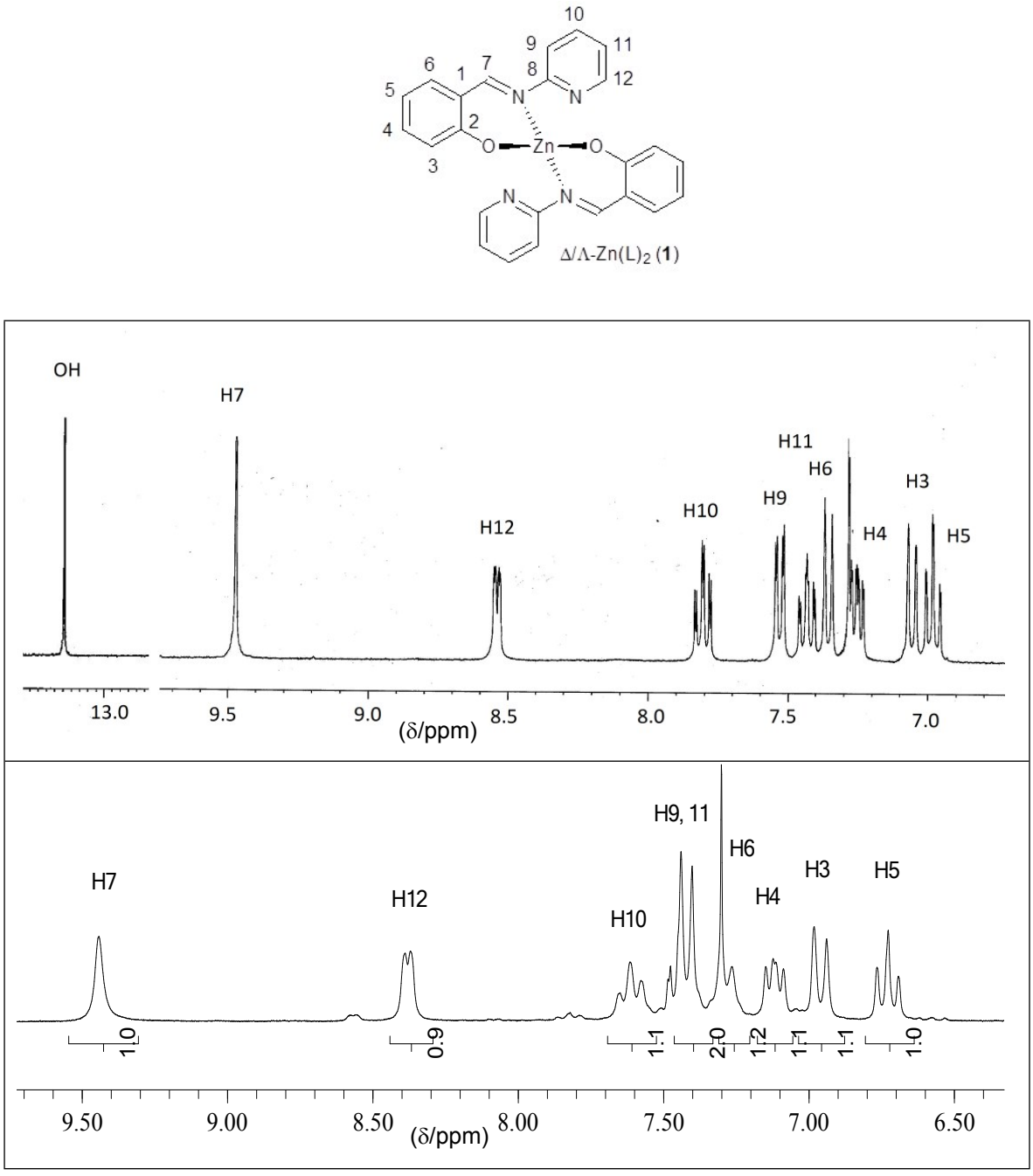

Fig. S1 [1]H NMR spectra of HL (top) and **1** (bottom) in $CDCl_3$ at 25 °C.

Cyclic voltammetry.

Cyclic voltammograms of HL and **1** were recorded in the range of –0.05 to 1.8 V *versus* Ag/AgCl in acetonitrile at varying scan rates (Figure S2). The anodic wave shows three peaks at potentials of *ca.* 0.70 V (E_a1), 1.00 V (E_a2) and 1.25 V (E_aHL) in the free Schiff base ligand (HL). The former two weak peaks are due the oxidation of the electrolytes, while the latter relatively strong peak is due to oxidation of the ligand.[8] The corresponding reduction peaks are not detected on the cathodic wave, indicating an irreversible oxidation process. These peaks shift to the higher potentials upon coordination to the metal ion in the complex. However, the cathodic wave at 0 to –0.50 V shows a weak reduction peak at *ca.* –0.30 V (E_c) (Figure S2) due to $[Zn(L)_2]/[Zn(L)_2]^-$ couple, which shifts to the lower potential and obscures by the decomposition peak of the electrolyte (TBAP) with faster scan rates. The weak reduction peak results from rapid chemical transformation and/or instability of the $[Zn(L)_2]^-$ species. However, the corresponding oxidation peak is not detected on the anodic wave, indicating an irreversible electrochemical process. Analyses of voltammograms at varying scan rates demonstrate that the anodic and cathodic peaks shift to the higher and lower potentials, respectively with faster scan rates (Figure S2), indicate a diffusion-controlled electrochemical process.[8]

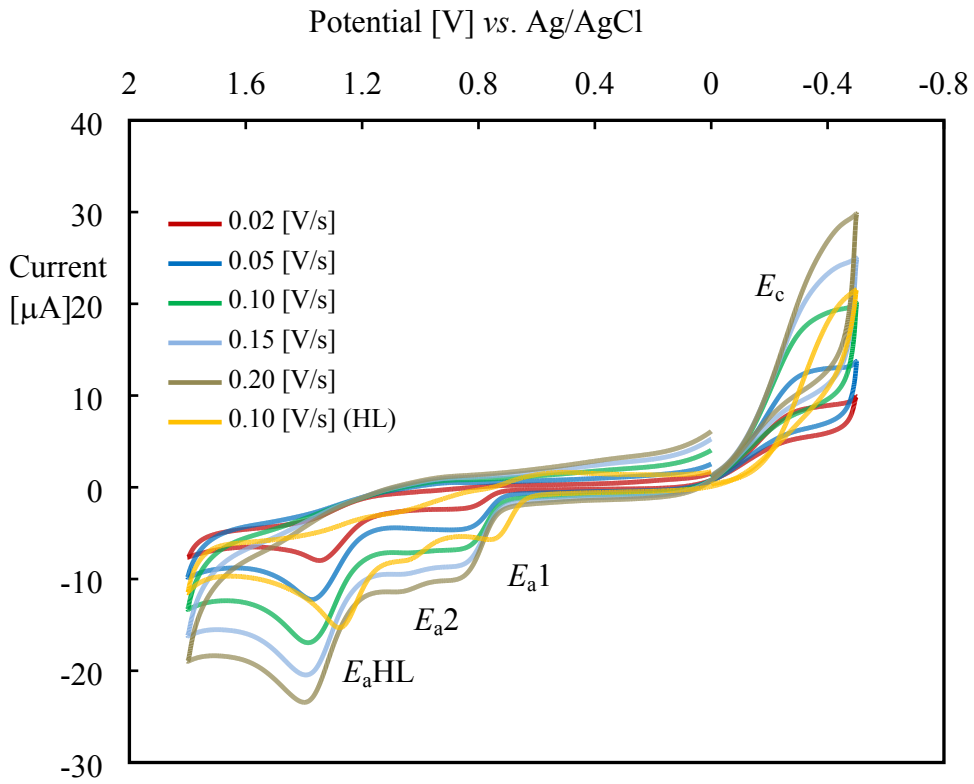

Fig. S2 Cyclic voltammograms of HL [1.5 mmol·dm^{-3}] and **1** [1.0 mmol·dm^{-3}]; TBAP [0.1 mol·dm^{-3}] at varying scan rates in acetonitrile at 25 °C**.**

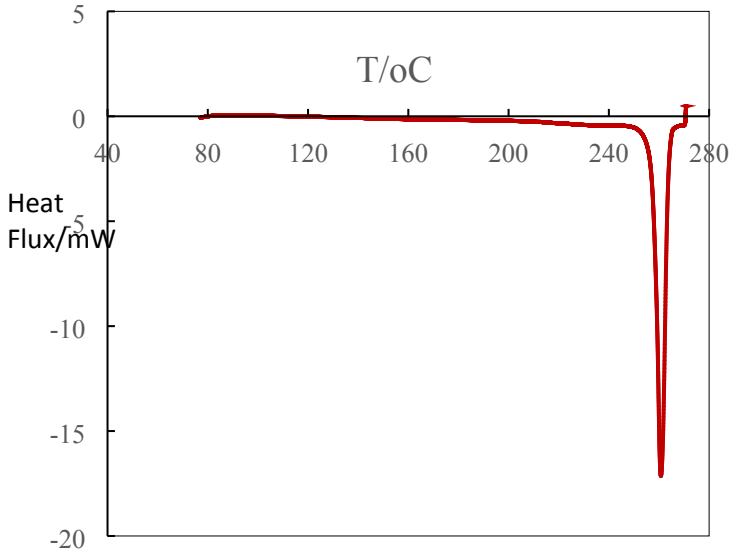

Fig. S3 DSC trace for compound **1**.

Electronic spectra and excited state properties.

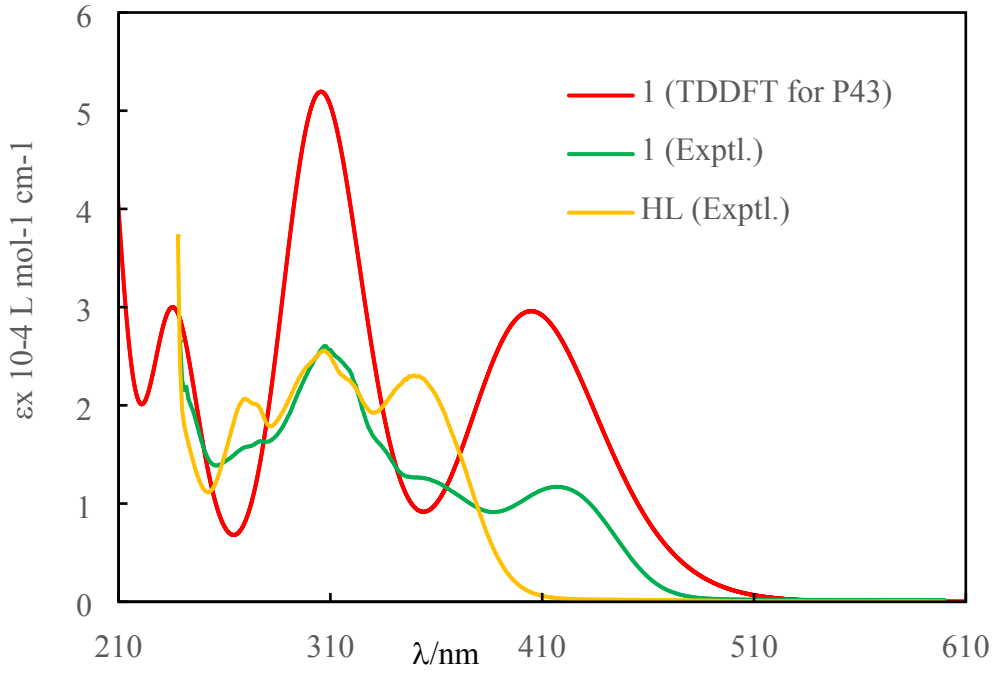

Fig. S4 Electronic spectra of HL (8.02×10^{-5} mol dm^{-3}) and **1** (9.11×10^{-5} mol dm^{-3}), and computed spectrum of **1** (calculated at B3LYP/TZVP//B3LYP/6-31G(d) for $P4_3$-enantiomer) in chloroform at 25 °C.

Excited state properties by TD-DFT were calculated at B3LYP/TZVP//B3LYP/6-31G(d) level of theory, incorporating PCM (Polarization Continuum Model) using chloroform as solvent. The computed electronic spectra for both $P4_1$(Δ)- and $P4_3$(Λ)-enantiomers are identical

and show the best fit to the experimental one (Figure S4). The selected and simplified spectral data, relevant to the experimental one, are listed in Table S1, and their assignments are made based on the orbital and population analyses.[9] The excited state properties (Table S7) demonstrate a large number of transitions at a single wave length (i.e., at a single excitation state). Thus, a combined metal-centered (MM), metal-ligand (ML) and ligand-centered (LL) transitions band appears at 414 nm (λ_{max}) with the highest molecular orbital (MO) contribution of 90% for HOMO (H) to LUMO (L) transitions, which is very close to the corresponding experimental band found at 416 nm (Table S1). The HOMO (H) and LUMO (L) are shown in Figure S6. Further, there are several bands/shoulders in the computed spectrum, which are comparable to the experimental bands (Table S1 and Figure S4).

Table S1 Selected and simplified spectral data, relevant to the experimental one, for **1a** ($P4_3$-enantiomer), calculated at B3LYP/TZVP//B3LYP/6-31G(d) in chloroform.

Wavelength [a] (nm)	Excitation energies	Oscillator strengths (f)	MO contributions (%) [b]	Assignments [c]
414 (416)	2.9942	0.0736	H→L (90)	MM, ML, LL
402	3.0873	0.2995	H-1→L+1 (90)	ML, LL
322 (316sh)	3.8557	0.1206	H-5→L (32), H-4→L+1 (31)	MM, ML, LL
307 (308)	4.0355	0.2478	H-3→L (90)	MM, ML, LL
236	5.2627	0.3714	H-1→L+7 (20), H→L+6 (70)	ML, LL

[a] Experimental values are in parentheses; [b] H = HOMO and L = LUMO; [c] MM = metal-centered, ML = metal-ligand and LL = ligand-centered transitions bands.

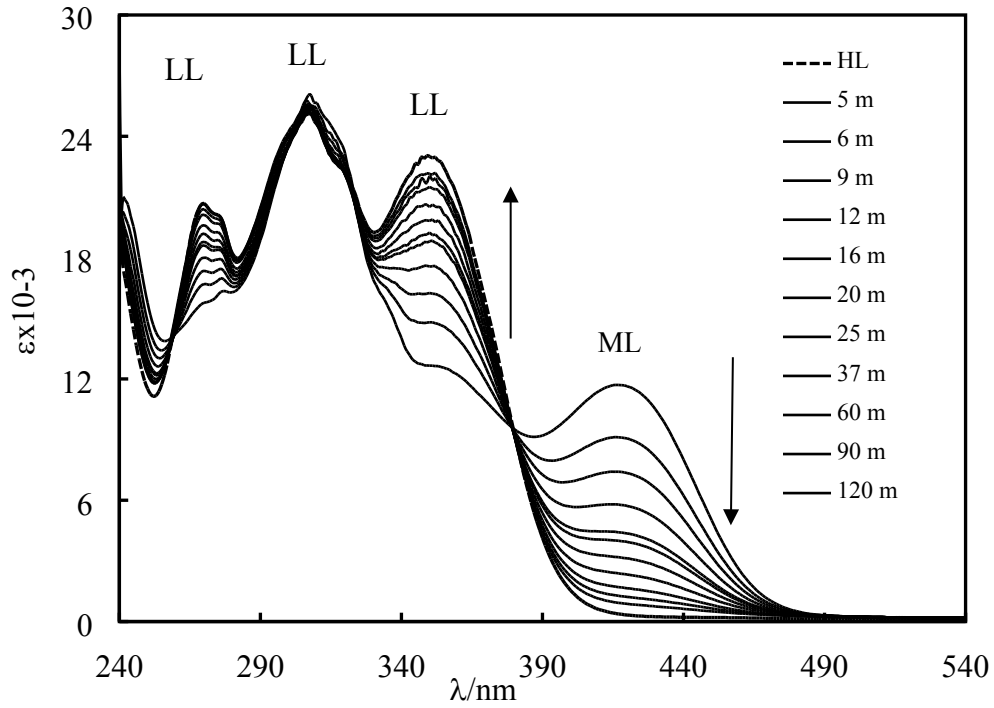

Fig. S5 Electronic spectra of **1** (9.11×10^{-5} mol·dm^{-3}) at different time intervals in chloroform at 25 °C (ML = metal-ligand and LL = ligand-centered transitions bands).

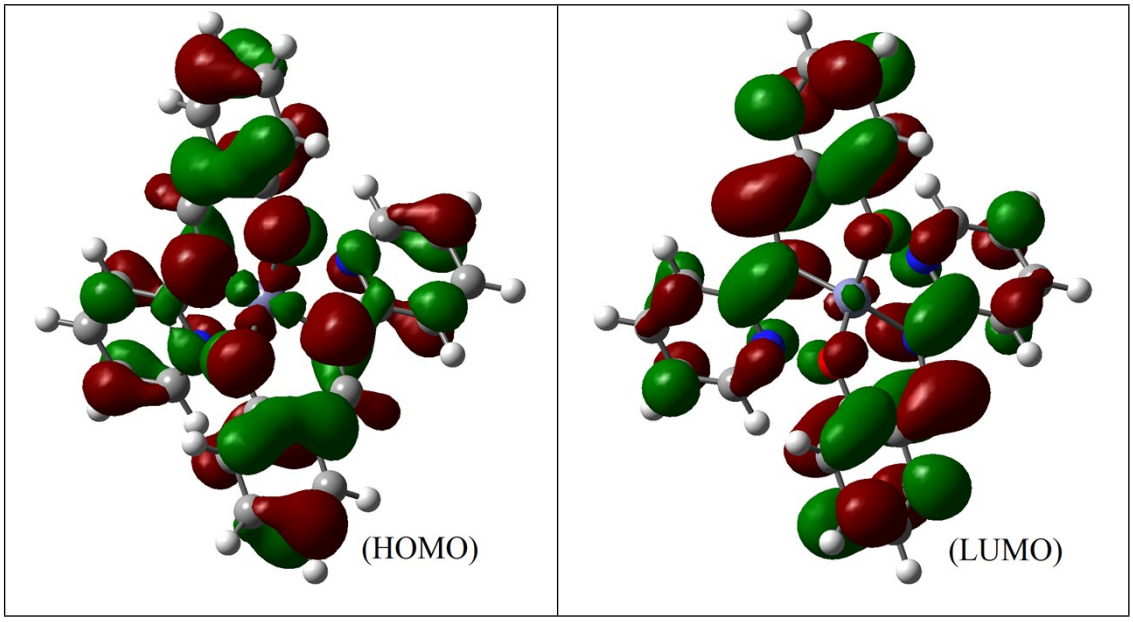

Fig. S6 The HOMO (H) and LUMO (L) for **1a** (for $P4_3$-enantiomer), calculated at B3LYP/TZVP//B3LYP/6-31G(d) in chloroform.

Single-crystal structural analyses.

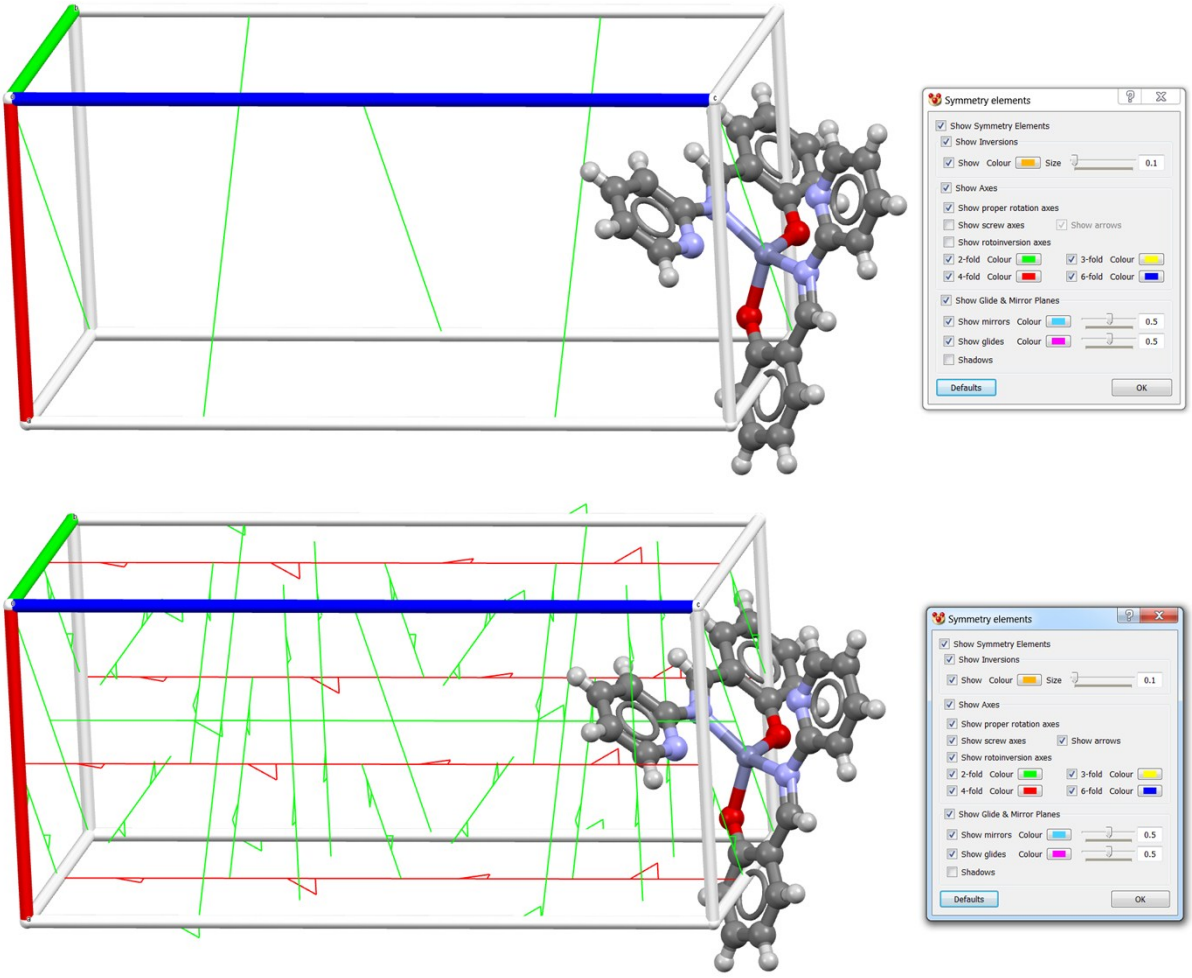

Fig. S7 (a) Selected 2-fold rotation axes (top) and (b) 4-fold rotation (or screw) axes (bottom), and full set of symmetry elements in the unit cell of the structure of **1**. Figures drawn with the program Mercury.[10]

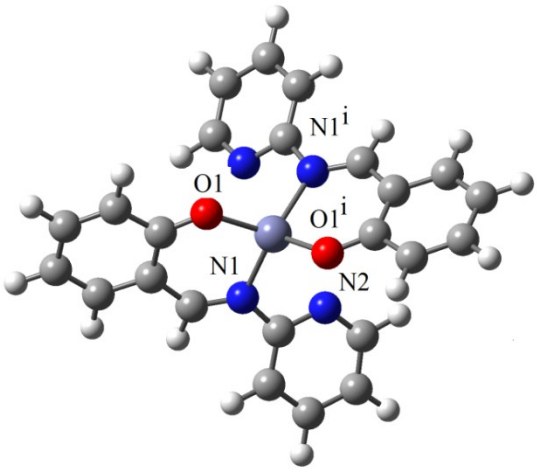

*P*4$_3$(Λ)-enantiomer (from data set **1a**)
(–3073.783627 au)

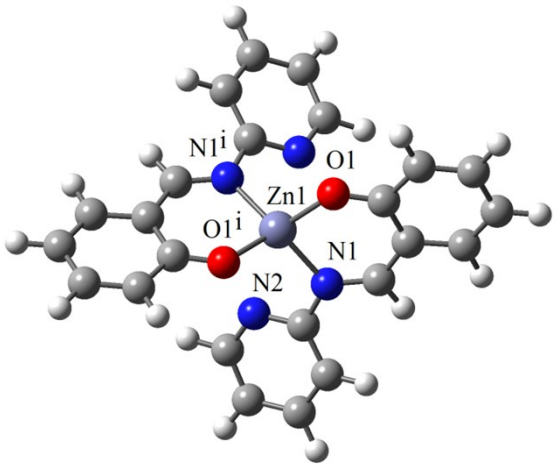

*P*4$_1$(Δ)-enantiomer (from data set **1d**)
(–3073.783631 au)

Fig. S8 Optimized structures by DFT for compound **1** at B3LYP/6-31G(d).

Table S2 Selected bond lengths (Å) and angles (°) in compound **1** [a].

Λ-structures in $P4_32_12$	Crystal **1a**	Crystal **1b**	Crystal **1c**	Crystal **1g**	Crystal **1h**	Opt. Struct. for **1a** [#]
Zn1-O1/ O1^{i}	1.961(1)	1.959(1)	1.962(1)	1.963(1)	1.9638(13)	1.938
Zn1-N1/ N1^{i}	1.999(1)	2.001(1)	2.002(1)	1.997(1)	1.9978(14)	2.011
Zn1-N2 / N2^{i}	2.823	2.817	2.819	2.813	2.816	2.935
O1-Zn1-O1^{i}	103.43(5)	103.43(5)	103.44(5)	102.41(7)	102.44(8)	114.28
O1-Zn1-N1	94.14(5)	94.21(5)	94.17(5)	94.27(5)	94.29(5)	94.24
O1^{i}-Zn1-N1	116.10(6)	116.01(5)	116.13(5)	116.11(5)	116.12(5)	112.09
N1-Zn1-N1^{i}	131.18(5)	131.19(4)	131.07(5)	131.51(8)	131.44(8)	131.01
Δ-structures in $P4_12_12$	Crystal **1d**	Crystal **1e**	Crystal **1f**	Opt. Struct. for **1d** [#]		
Zn1-O1/ O1^{i}	1.956(1)	1.961(1)	1.959(1)	1.9377		
Zn1-N1/ N1^{i}	2.000(1)	1.992(1)	1.995(1)	2.0107		
Zn1-N2 / N2^{i}	2.818	2.810	2.813	2.936		
O1-Zn1-O1^{i}	103.52(5)	102.19(4)	102.25(5)	114.31		
O1-Zn1-N1	94.16(5)	94.28(5)	94.37(5)	94.25		
O1^{i}-Zn1-N1	116.08(5)	116.17(5)	116.07(5)	112.09		
N1-Zn1-N1^{i}	131.13(5)	131.52(5)	131.49(5)	130.96		

[a] Symmetry transformation (i) *y*, *x*, -*z*+2 or *y*, *x*, -*z*+1
[#] Optimized structures using the cif-files from experimental measurements.

Table S3 Assignments of distortions from tetrahedral to square-planar geometry in **1**.

Crystals	Space group	Left (*M*)- or right (*P*)-handed helices	Induced Δ- or Λ-chirality at-metal center	θ/° [a] (Opt. Struct.) [#]	$\tau_{tet\text{-}sq} = \theta/90°$ (Opt. Struct.) [#]	τ_4 [b] (Opt. Struct.) [#]
1a	$P4_32_12$	*M*	Λ	87.66 (82.58)	0.974 (0.918)	0.799 (0.814)
1b	$P4_32_12$	*M*	Λ	87.73	0.975	0.800
1c	$P4_32_12$	*M*	Λ	87.62	0.974	0.800
1g	$P4_32_12$	*M*	Λ	87.04	0.967	0.797
1d	$P4_12_12$	*P*	Δ	87.73 (82.58)	0.975 (0.918)	0.800 (0.814)
1e	$P4_12_12$	*P*	Δ	86.86	0.965	0.797
1f	$P4_12_12$	*P*	Δ	86.97	0.966	0.797
1h	$P4_32_12$	*M*	Λ	87.04	0.967	0.797

[a] Calculated with Diamond[11] according to the Scheme 3.
[b] See Table S2 for the two largest angles, α and β.
[#] Values in parentheses are calculated from DFT Optimized Structures.

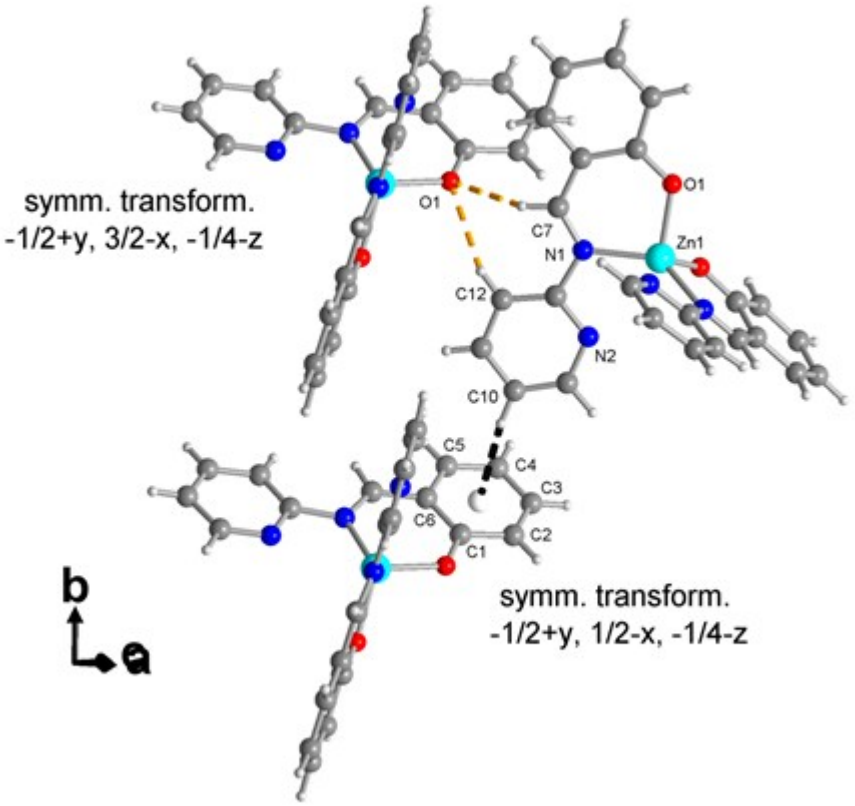

Fig. S9. Summary of unique and significant C–H···π contact (dashed black line) and C–H···O hydrogen bonds (dashed yellow lines) between adjacent molecules in the crystal packing of **1** (from data set **1e**). For details see Table S4, S5 and S6.

Hirshfeld surface analyses.

H...O and O...H contacts (reciprocal contributions are almost equal 5.4 and 5.7): 11.1 %

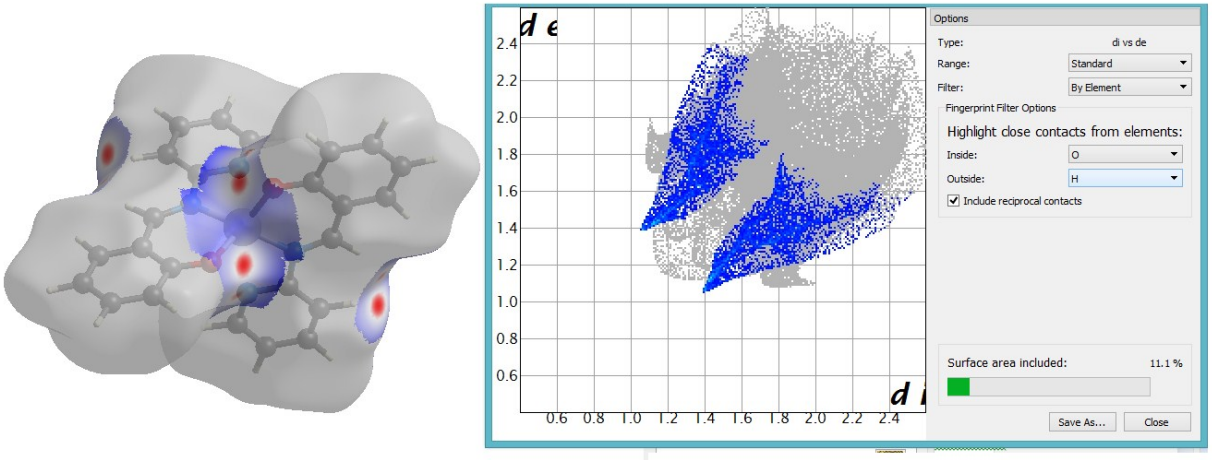

H...C and C...H contacts (reciprocal contributions are not equal, 17.3 and 23.4): 40.7 %

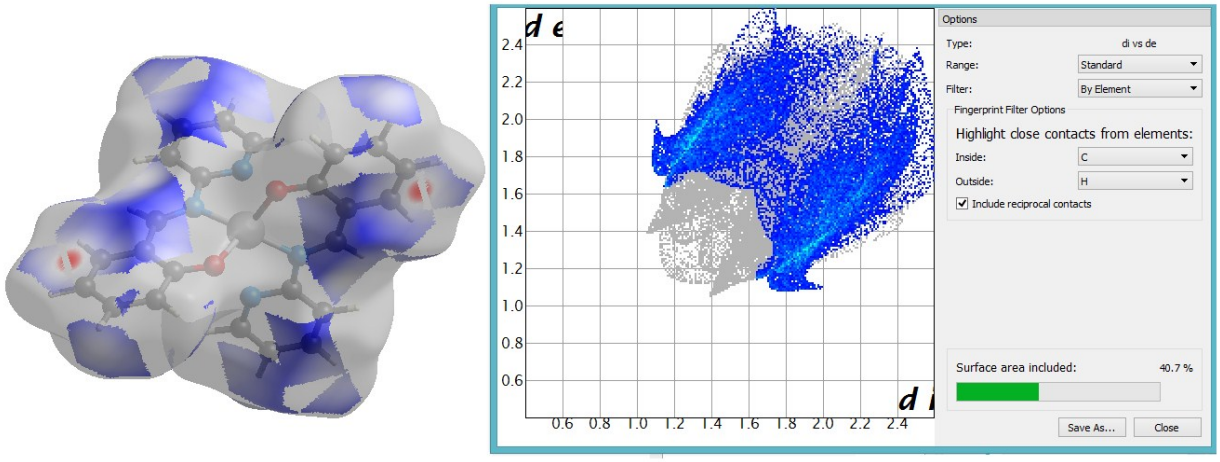

H...H contacts: 38.9 %

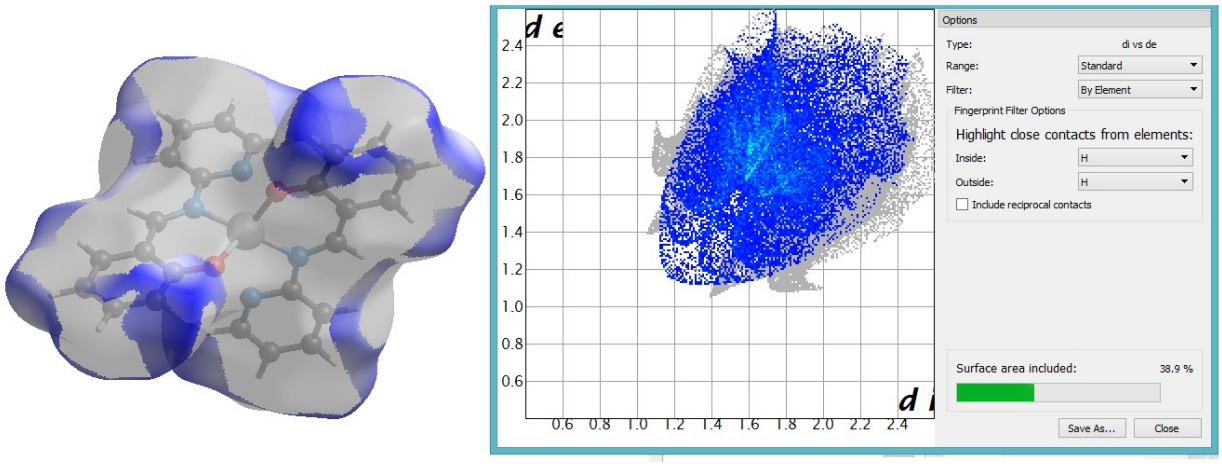

C...C contacts: 1.2 %

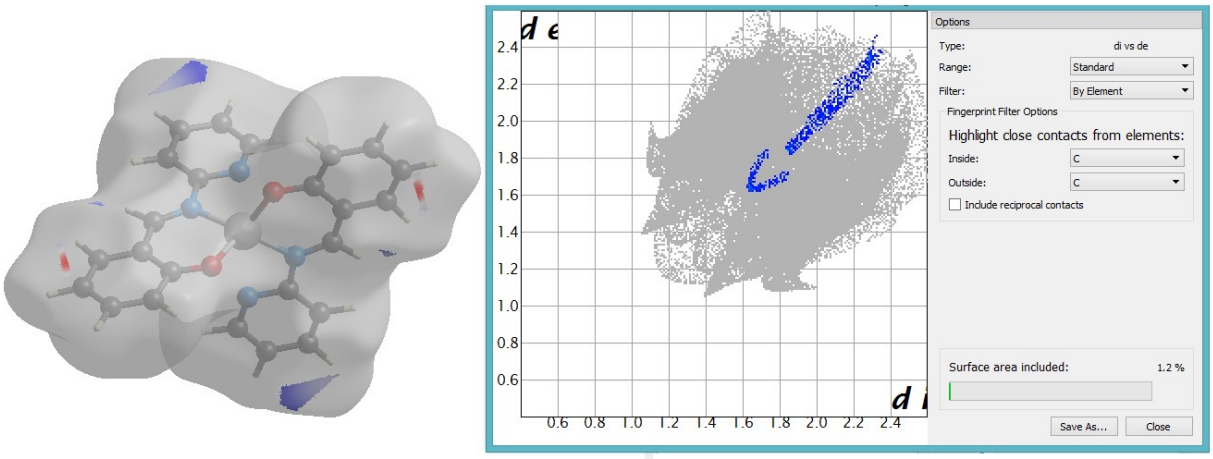

Fig. S10 Breakdown of Hirshfeld surface of the 2D fingerprint plot into the contributions from O···H, C···H, C···C, and H···H close intermolecular contacts, respectively.

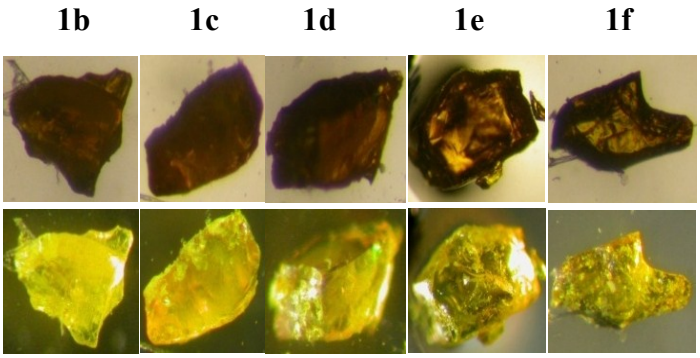

Fig. S11 Crystals photos of different crystals compound **1**. The upper images were taken by shining light through the crystals from below. The lower images were obtained by shining light on top of the crystals.

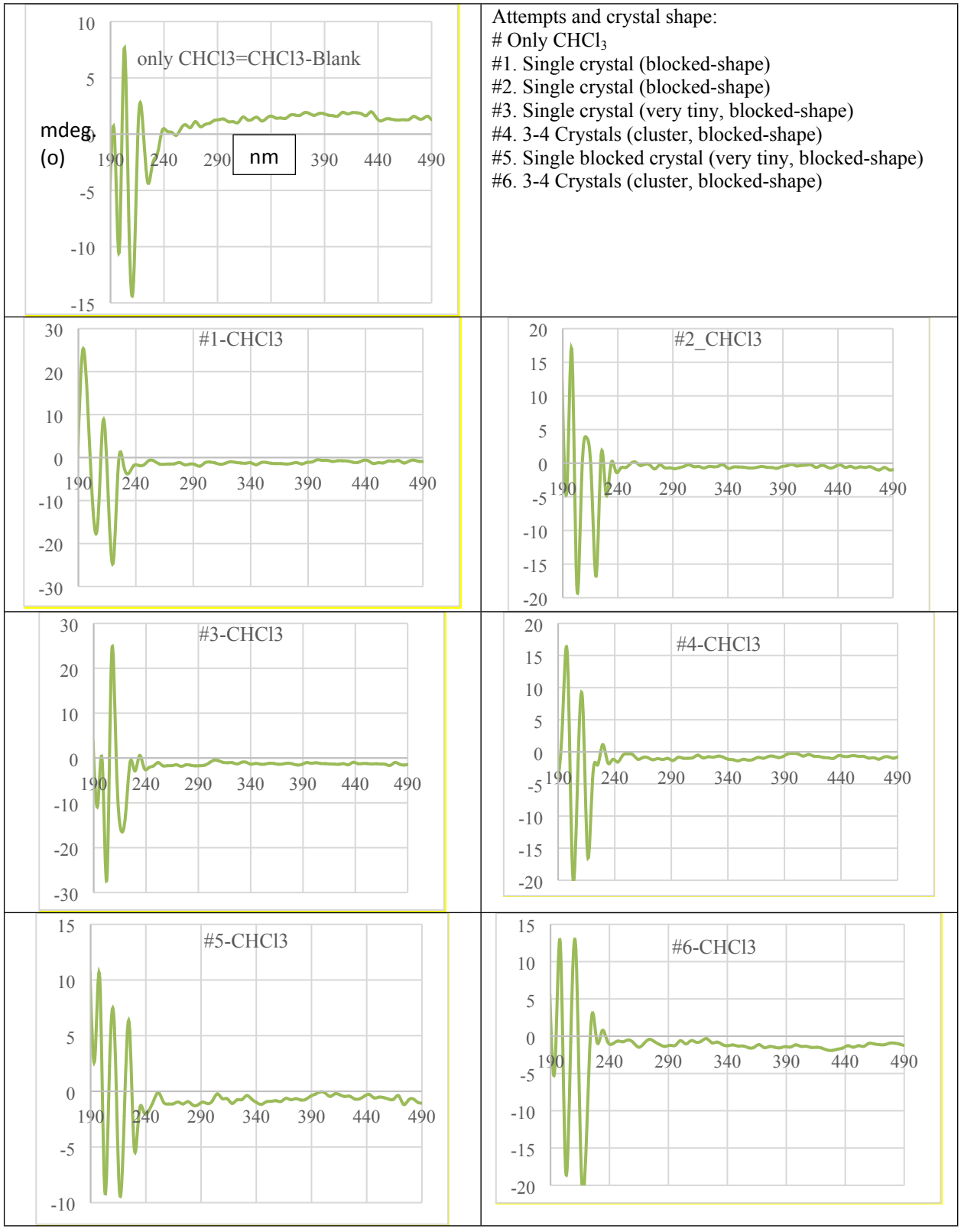

Fig. S12 ECD spectra of one or a few single crystals of compound **1** in chloroform (0.1 mL, sufficient color, arbitrary concentration) at 20 °C; cell path length 1.0 mm. Each abscissa scale from 190 to 490 is in nm, each ordinate scale is in degree (°).

Packing analyses.

Significant intermolecular C-H···π contacts start below around 2.7 Å for the (C-)H···ring centroid distances with H-perp also starting at below 2.6-2.7 Å and C-H···Cg > 145°.[12]

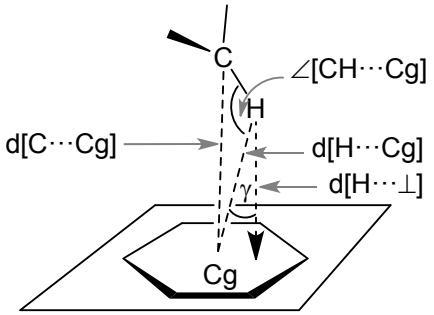

Scheme S1. Graphical presentation of the parameters used for the description of C-H…π interactions.

Table S4 Analysis of intermolecular C-H...Cg(π-ring) interactions (H..Cg < 3.0 Ang. - Gamma < 30.0 Deg) in **1** (data set **1e**).

- Cg(J) = Center of gravity of ring J (Plane number above)
- H-Perp = Perpendicular distance of H to ring plane J
- Gamma = Angle between Cg-H vector and ring J normal
- C-H..Cg = C-H-Cg angle (degrees)
- C..Cg = Distance of X to Cg (Angstrom)
- C-H, Pi = Angle of the X-H bond with the Pi-plane (i.e.' Perpendicular = 90 degrees, Parallel = 0 degrees)

C--H(I)	Cg(J)	[ARU(J)]	H..Cg	H-Perp	Gamma	C-H..Cg	C..Cg	C-H,Pi
C(10)-H(10)	> Cg(4)	[4454.01]	2.611(19)	2.60	4.35	151.9(15)	3.458(2)	58

[4454] = -1/2+Y,1/2-X,-1/4+Z

The Cg(I) refer to the Ring Centre-of-Gravity numbers given in Cg(4) = Ring C1-C2-C3-C4-C5-C6

Table S5 C-H···O Hydrogen-bond geometry (Å, °) in **1** (data set **1e**).[a]

==========

Analysis of Potential Hydrogen Bonds and Schemes with d(D...A) < R(D)+R(A)+0.50, d(H...A) < R(H)+R(A)-0.12 Ang., D-H...A > 100.0 Deg

==========

Note: - ARU codes in [ ] are with reference to the Coordinates printed above (Possibly transformed, when MOVE .NE. 1.555)

==========

D --- H....A	[ARU]	D - H	H...A	D...A	D - H...A
C(7)--H(7) ..O(1)	[4464.01]	0.933(16)	2.532(15)	3.294(2)	139.0(13)
C(12)--H(12) ..O(1)	[4464.01]	0.903(18)	2.568(18)	3.389(2)	151.4(15)

[4464.] = [3_464] = -1/2+y,3/2-x,-1/4+z

[a] D = Donor, A = Acceptor. For found and refined H atoms the standard deviations are given for their hydrogen bond distances and angles.

Table S6 Intermolecular hydrogen bonding interactions with lengths (Å) and angles (°) in data set **1a - 1g**.[a]

data set #	D-H···A	d(D-H)	d(H···A)	d(D···A)	<(DHA)
1a	C7-H7···O1^{i}	0.94(2)	2.633(17)	3.381(2)	137(2)
	C12-H12···O1^{i}	0.88(3)	2.65(3)	3.427(2)	148(2)
1b	C7-H7···O1^{i}	0.96(2)	2.64(2)	3.382(2)	135(2)
	C12-H12···O1^{i}	0.85(3)	2.63(3(	3.425(2)	155(3)
1c	C7-H7···O1^{i}	0.96(2)	2.62(2)	3.379(2)	137(2)
	C12-H12···O1^{i}	0.88(3)	2.64(3)	3.429(2)	151(3)
1d	C7-H7···O1^{i}	0.96(2)	2.62(2)	3.381(2)	136(2)
	C12-H12···O1^{i}	0.85(2)	2.65(3)	3.430(2)	152(3)
1e	C7-H7···O1^{i}	0.93(2)	2.532(15)	3.294(2)	139(2)
	C12-H12···O1^{i}	0.90(2)	2.568(18)	3.389(2)	151(2)
1f	C7-H7···O1^{i}	0.94(2)	2.585(19)	3.305(2)	134(2)
	C12-H12···O1^{i}	0.94(2)	2.550(2)	3.392(2)	149(2)
1g	C7-H7···O1^{i}	0.95	2.55	3.317(2)	138
	C12-H12···O1^{i}	0.95	2.55	3.393(2)	151

[a] Symmetry operations for **1a**: i = 1/2-y, 1/2+x, -1/4+z.

Symmetry operations for **1b**: i = 1/2+y, 1/2-x, 1/4+z.

Symmetry operations for **1c**: i = 1/2-y, -1/2+x, -1/4+z.

Symmetry operations for **1d**: i = 1.5-y, -1/2+x, 1/4-z.

Symmetry operations for **1e**: i = -1/2+y, 3/2-x,-1/4+z.

Symmetry operations for **1f**: i = 3/2-y, -1/2+x, 1/4+z.

Symmetry operations for **1g**: i = 3/2-y, -1/2+x, -1/4+z

Excitation properties.

Table S7 Calculated excited states and their corresponding MO contributions, excitation energy (eV), Wavelength (nm) and Osilator Strenth (f) for compound **1** with $P4_3(\Lambda)$-form at B3LYP/TZVP// B3LYP/6-31g(d) level of theory in chloroform.

Excitation energies and oscillator strengths.

```
Excited State   1:      Singlet-B      2.9942 eV  414.09 nm  f=0.0736  <S**2>=0.000
    117 ->120         0.20955
    118 ->119         0.67159
This state for optimization and/or second-order correction.
Total Energy, E(TD-HF/TD-KS) =  -3074.70959918
Copying the excited state density for this state as the 1-particle RhoCI density.

Excited State   2:      Singlet-A      2.9977 eV  413.60 nm  f=0.0569  <S**2>=0.000
    117 ->119         0.67962
    118 ->120         0.18265

Excited State   3:      Singlet-A      3.0683 eV  404.07 nm  f=0.1618  <S**2>=0.000
    117 ->119        -0.18224
    118 ->120         0.67920

Excited State   4:      Singlet-B      3.0873 eV  401.59 nm  f=0.2995  <S**2>=0.000
    117 ->120         0.67080
    118 ->119        -0.20830

Excited State   5:      Singlet-A      3.8229 eV  324.32 nm  f=0.0349  <S**2>=0.000
    113 ->120        -0.29363
    114 ->119         0.39454
    115 ->120         0.13161
    116 ->119         0.47647

Excited State   6:      Singlet-B      3.8557 eV  321.56 nm  f=0.1206  <S**2>=0.000
    113 ->119         0.39959
    114 ->120        -0.39076
    115 ->119        -0.18546
    116 ->120        -0.37221

Excited State   7:      Singlet-B      4.0355 eV  307.23 nm  f=0.2478  <S**2>=0.000
    115 ->119         0.66718
    116 ->120        -0.20262

Excited State   8:      Singlet-A      4.0441 eV  306.58 nm  f=0.0524  <S**2>=0.000
    113 ->120         0.31607
    114 ->119        -0.33795
    115 ->120        -0.10678
    116 ->119         0.50950

Excited State   9:      Singlet-B      4.0757 eV  304.20 nm  f=0.2514  <S**2>=0.000
    113 ->119        -0.23232
    114 ->120         0.12603
    116 ->120        -0.36176
    118 ->121         0.53378

Excited State  10:      Singlet-A      4.0834 eV  303.63 nm  f=0.0988  <S**2>=0.000
    114 ->119        -0.12776
    115 ->120         0.62015
    117 ->121         0.20966
    118 ->122        -0.20480

Excited State  11:      Singlet-B      4.0851 eV  303.50 nm  f=0.2025  <S**2>=0.000
    113 ->119         0.27271
    114 ->120        -0.14849
    116 ->120         0.40841
```

```
    117 ->122         0.13386
    118 ->121         0.45359

Excited State  12:      Singlet-A      4.0919 eV  303.00 nm  f=0.0002  <S**2>=0.000
    115 ->120        -0.16615
    117 ->121         0.66683
    118 ->122         0.13596

Excited State  13:      Singlet-A      4.1307 eV  300.15 nm  f=0.0258  <S**2>=0.000
    115 ->120         0.22203
    118 ->122         0.65354

Excited State  14:      Singlet-B      4.1390 eV  299.55 nm  f=0.0138  <S**2>=0.000
    117 ->122         0.68789

Excited State  15:      Singlet-A      4.3523 eV  284.87 nm  f=0.0069  <S**2>=0.000
    113 ->120         0.54756
    114 ->119         0.43888

Excited State  16:      Singlet-B      4.3561 eV  284.62 nm  f=0.0812  <S**2>=0.000
    113 ->119         0.44124
    114 ->120         0.53952

Excited State  17:      Singlet-B      4.4378 eV  279.38 nm  f=0.0041  <S**2>=0.000
    109 ->120         0.13576
    111 ->120         0.21307
    112 ->119         0.64867

Excited State  18:      Singlet-A      4.4784 eV  276.85 nm  f=0.0037  <S**2>=0.000
    109 ->119         0.18309
    111 ->119         0.30835
    112 ->120         0.59491

Excited State  19:      Singlet-A      4.7288 eV  262.19 nm  f=0.0003  <S**2>=0.000
    109 ->119         0.17630
    111 ->119         0.56414
    112 ->120        -0.35154

Excited State  20:      Singlet-B      4.7611 eV  260.41 nm  f=0.0071  <S**2>=0.000
    109 ->120         0.14537
    110 ->119         0.17718
    111 ->120         0.55732
    112 ->119        -0.22453
    117 ->124         0.18661
    118 ->123         0.18833

Excited State  21:      Singlet-A      4.8012 eV  258.24 nm  f=0.0026  <S**2>=0.000
    109 ->119         0.30071
    110 ->120        -0.21646
    117 ->123         0.38921
    118 ->124         0.41237

Excited State  22:      Singlet-B      4.8042 eV  258.07 nm  f=0.0219  <S**2>=0.000
    109 ->120        -0.28656
    110 ->119         0.25307
    111 ->120        -0.20774
    112 ->119         0.13524
    117 ->124         0.26327
    118 ->123         0.44152

Excited State  23:      Singlet-A      4.8905 eV  253.52 nm  f=0.0001  <S**2>=0.000
    117 ->123         0.50409
    118 ->124        -0.48581

Excited State  24:      Singlet-B      4.8930 eV  253.39 nm  f=0.0086  <S**2>=0.000
    117 ->124         0.55087
    118 ->123        -0.42453

Excited State  25:      Singlet-B      4.9402 eV  250.97 nm  f=0.0022  <S**2>=0.000
    107 ->120         0.17148
```

```
    108 ->119        -0.20810
    109 ->120         0.10639
    110 ->119        -0.29562
    115 ->121         0.29964
    116 ->122         0.33626
    117 ->124         0.20425
    118 ->123         0.22157

Excited State  26:      Singlet-A      4.9407 eV  250.94 nm  f=0.0000  <S**2>=0.000
    107 ->119         0.21123
    108 ->120        -0.18386
    109 ->119         0.17232
    110 ->120        -0.12564
    115 ->122         0.28116
    116 ->121         0.43804
    117 ->123        -0.17231
    118 ->124        -0.19602

Excited State  27:      Singlet-B      5.0008 eV  247.93 nm  f=0.0236  <S**2>=0.000
    109 ->120         0.20535
    110 ->119         0.54266
    111 ->120        -0.13682
    115 ->121         0.23210
    116 ->122         0.19648
    117 ->124        -0.10243

Excited State  28:      Singlet-A      5.0198 eV  246.99 nm  f=0.0013  <S**2>=0.000
    109 ->119         0.50816
    110 ->120         0.36299
    111 ->119        -0.25634
    116 ->121        -0.14999

Excited State  29:      Singlet-A      5.0656 eV  244.76 nm  f=0.0128  <S**2>=0.000
    109 ->119        -0.17270
    110 ->120         0.51900
    116 ->121         0.31652
    117 ->123         0.16767
    118 ->124         0.16609

Excited State  30:      Singlet-B      5.0831 eV  243.92 nm  f=0.0436  <S**2>=0.000
    109 ->120         0.54333
    111 ->120        -0.25544
    115 ->121        -0.22385
    116 ->122        -0.15797
    117 ->124         0.14331
    118 ->123         0.10754

Excited State  31:      Singlet-B      5.1350 eV  241.45 nm  f=0.0027  <S**2>=0.000
    111 ->122         0.15206
    112 ->121         0.22490
    115 ->121        -0.43874
    116 ->122         0.46023

Excited State  32:      Singlet-A      5.1436 eV  241.05 nm  f=0.0005  <S**2>=0.000
    111 ->121        -0.17315
    112 ->122        -0.21353
    114 ->121        -0.10613
    115 ->122         0.52618
    116 ->121        -0.31845

Excited State  33:      Singlet-B      5.1779 eV  239.45 nm  f=0.0073  <S**2>=0.000
    109 ->122         0.19555
    111 ->122         0.32106
    112 ->121         0.49412
    115 ->121         0.19152
    116 ->122        -0.22751

Excited State  34:      Singlet-A      5.1927 eV  238.77 nm  f=0.0094  <S**2>=0.000
    109 ->121         0.21233
    111 ->121         0.33340
```

```
    112 ->122         0.47633
    115 ->122         0.22140
    116 ->121        -0.17708

Excited State  35:      Singlet-B      5.2627 eV  235.59 nm  f=0.3714  <S**2>=0.000
    117 ->126        -0.31384
    118 ->125         0.59282

Excited State  36:      Singlet-A      5.2686 eV  235.33 nm  f=0.0563  <S**2>=0.000
    117 ->125         0.57408
    118 ->126        -0.31820

Excited State  37:      Singlet-A      5.2937 eV  234.21 nm  f=0.0028  <S**2>=0.000
    117 ->125         0.35846
    118 ->126         0.59560

Excited State  38:      Singlet-B      5.2948 eV  234.16 nm  f=0.0327  <S**2>=0.000
    117 ->126         0.60576
    118 ->125         0.34189

Excited State  39:      Singlet-A      5.4062 eV  229.34 nm  f=0.0004  <S**2>=0.000
    107 ->119        -0.23105
    108 ->120         0.10994
    114 ->121         0.62015
    115 ->122         0.16424

Excited State  40:      Singlet-B      5.4253 eV  228.53 nm  f=0.0103  <S**2>=0.000
    108 ->119         0.46352
    113 ->121         0.19984
    114 ->122         0.40523
    115 ->121         0.19640
    116 ->122         0.11978

Excited State  41:      Singlet-B      5.4658 eV  226.84 nm  f=0.0033  <S**2>=0.000
    113 ->121         0.65049
    114 ->122        -0.22361

Excited State  42:      Singlet-A      5.4693 eV  226.69 nm  f=0.0039  <S**2>=0.000
    107 ->119         0.57901
    111 ->121        -0.10144
    113 ->122        -0.11839
    114 ->121         0.27005
    115 ->122        -0.15364
    116 ->121        -0.13377

Excited State  43:      Singlet-B      5.4740 eV  226.50 nm  f=0.0086  <S**2>=0.000
    107 ->120        -0.24483
    108 ->119        -0.43404
    113 ->121         0.10968
    114 ->122         0.46937

Excited State  44:      Singlet-A      5.4998 eV  225.43 nm  f=0.0015  <S**2>=0.000
    107 ->119         0.16123
    108 ->120         0.41886
    113 ->122         0.50457
    115 ->122         0.10297

Excited State  45:      Singlet-A      5.5171 eV  224.73 nm  f=0.0000  <S**2>=0.000
    108 ->120         0.47207
    113 ->122        -0.46291
    114 ->121        -0.11150
    115 ->122         0.11374
    116 ->121         0.10172

Excited State  46:      Singlet-B      5.5351 eV  223.99 nm  f=0.0509  <S**2>=0.000
    107 ->120         0.59917
    110 ->121        -0.10888
    114 ->122         0.22263
    115 ->121        -0.14144
    116 ->122        -0.15126
```

```
Excited State  47:      Singlet-A      5.8178 eV  213.11 nm  f=0.0207  <S**2>=0.000
    103 ->119        -0.13380
    104 ->120         0.16888
    105 ->120         0.10435
    106 ->119         0.21194
    113 ->124         0.15520
    114 ->123         0.17913
    115 ->124        -0.12868
    116 ->123         0.44496
    117 ->127        -0.25597
    118 ->128         0.15565

Excited State  48:      Singlet-B      5.8210 eV  212.99 nm  f=0.0327  <S**2>=0.000
    103 ->120         0.17426
    104 ->119        -0.24352
    105 ->119        -0.24740
    106 ->120        -0.17293
    113 ->123         0.16622
    114 ->124         0.19608
    115 ->123        -0.13809
    116 ->124         0.41822
    117 ->128         0.15583
    118 ->127        -0.10243

Excited State  49:      Singlet-B      5.8630 eV  211.47 nm  f=0.0946  <S**2>=0.000
    103 ->120        -0.14982
    104 ->119         0.13124
    105 ->119         0.34940
    115 ->123        -0.20126
    115 ->125        -0.18378
    116 ->124         0.10351
    116 ->126        -0.24034
    117 ->128         0.19706
    118 ->127        -0.33599

Excited State  50:      Singlet-A      5.8952 eV  210.31 nm  f=0.0106  <S**2>=0.000
    103 ->119        -0.26592
    104 ->120         0.24878
    105 ->120         0.35253
    106 ->119         0.18942
    113 ->126         0.13826
    114 ->125        -0.13879
    115 ->126        -0.10453
    116 ->123        -0.24586
    116 ->125        -0.14346
    118 ->128        -0.14908

Excited State  51:      Singlet-B      5.9091 eV  209.82 nm  f=0.0121  <S**2>=0.000
    104 ->119         0.16717
    105 ->119         0.12108
    106 ->120         0.15226
    114 ->124         0.10813
    115 ->123         0.42041
    116 ->124         0.43005

Excited State  52:      Singlet-A      5.9118 eV  209.72 nm  f=0.0065  <S**2>=0.000
    105 ->120         0.15816
    106 ->119        -0.15905
    114 ->123         0.17246
    115 ->124         0.42752
    115 ->126        -0.12930
    116 ->123         0.30844
    116 ->125        -0.17908
    117 ->127         0.18673
    118 ->128        -0.17829

Excited State  53:      Singlet-A      5.9552 eV  208.19 nm  f=0.0017  <S**2>=0.000
    109 ->121         0.13860
    111 ->121         0.49944
```

```
    112 ->122        -0.43011
    115 ->124         0.12699

Excited State  54:      Singlet-B      5.9555 eV  208.18 nm  f=0.0203  <S**2>=0.000
    109 ->122         0.16463
    110 ->121         0.10120
    111 ->122         0.50434
    112 ->121        -0.42073

Excited State  55:      Singlet-A      5.9693 eV  207.70 nm  f=0.0000  <S**2>=0.000
    106 ->119        -0.13463
    113 ->124         0.21921
    113 ->126        -0.28475
    114 ->123         0.31291
    114 ->125         0.29181
    115 ->124        -0.24689
    116 ->123        -0.16144
    117 ->127         0.15321

Excited State  56:      Singlet-B      5.9706 eV  207.66 nm  f=0.0367  <S**2>=0.000
    113 ->123        -0.28698
    113 ->125        -0.30107
    114 ->124        -0.25079
    114 ->126         0.33482
    115 ->123         0.16311
    116 ->124         0.16062
    116 ->126         0.10633
    117 ->128         0.14366
    118 ->127        -0.18808

Excited State  57:      Singlet-A      6.0003 eV  206.63 nm  f=0.0002  <S**2>=0.000
    105 ->120        -0.11966
    106 ->119         0.32315
    109 ->121        -0.16369
    113 ->126        -0.14757
    114 ->125         0.15366
    115 ->124         0.35297
    115 ->126         0.16745
    116 ->123        -0.14345
    116 ->125         0.25076

Excited State  58:      Singlet-B      6.0071 eV  206.40 nm  f=0.0673  <S**2>=0.000
    104 ->119        -0.15307
    106 ->120        -0.27681
    109 ->122         0.15621
    110 ->121        -0.24319
    115 ->123         0.38010
    115 ->125        -0.18365
    116 ->124        -0.13813
    116 ->126        -0.22668

Excited State  59:      Singlet-A      6.0757 eV  204.07 nm  f=0.0181  <S**2>=0.000
    106 ->119         0.16337
    107 ->119        -0.12381
    107 ->123        -0.11041
    108 ->120         0.13073
    108 ->124        -0.10939
    109 ->121         0.45038
    110 ->122        -0.33812
    111 ->121        -0.10585
    113 ->124         0.11477

Excited State  60:      Singlet-B      6.0765 eV  204.04 nm  f=0.0113  <S**2>=0.000
    106 ->120        -0.17512
    107 ->120         0.13922
    107 ->122         0.10173
    107 ->124        -0.10286
    108 ->119        -0.11910
    109 ->122        -0.17638
    110 ->121         0.46287
```

```
    111 ->124         0.11427
    112 ->123        -0.15546
    113 ->123         0.14486
    115 ->123         0.12384
    116 ->124        -0.12288

Excited State  61:      Singlet-B      6.0973 eV  203.34 nm  f=0.0205  <S**2>=0.000
    105 ->119         0.13641
    109 ->124         0.11789
    110 ->121        -0.26360
    111 ->122         0.12454
    111 ->124         0.18529
    112 ->123        -0.30565
    113 ->123         0.16491
    113 ->125        -0.17511
    114 ->124         0.30584
    114 ->126         0.19930
    116 ->126         0.11263

Excited State  62:      Singlet-A      6.0979 eV  203.32 nm  f=0.0102  <S**2>=0.000
    105 ->120         0.12008
    109 ->121         0.11685
    109 ->123        -0.14407
    111 ->123        -0.23851
    112 ->124         0.40800
    113 ->124        -0.20455
    113 ->126        -0.16177
    114 ->123        -0.21705
    114 ->125         0.19109

Excited State  63:      Singlet-B      6.1314 eV  202.21 nm  f=0.1257  <S**2>=0.000
    105 ->119         0.22157
    106 ->120        -0.12482
    112 ->123         0.10547
    115 ->123        -0.10078
    117 ->128         0.30966
    118 ->127         0.49744
    118 ->130         0.11781

Excited State  64:      Singlet-A      6.1411 eV  201.89 nm  f=0.0002  <S**2>=0.000
    109 ->121         0.33494
    110 ->122         0.42824
    111 ->121        -0.19035
    113 ->124        -0.10363
    114 ->123        -0.10455
    117 ->127         0.24146
    118 ->128         0.20189

Excited State  65:      Singlet-A      6.1454 eV  201.75 nm  f=0.0015  <S**2>=0.000
    109 ->121        -0.17015
    110 ->122        -0.34980
    111 ->121         0.10020
    114 ->123        -0.11295
    117 ->127         0.37644
    118 ->128         0.35279

Excited State  66:      Singlet-B      6.1533 eV  201.49 nm  f=0.0005  <S**2>=0.000
    109 ->122         0.55913
    110 ->121         0.28406
    111 ->122        -0.25209

Excited State  67:      Singlet-B      6.1732 eV  200.84 nm  f=0.1597  <S**2>=0.000
    109 ->124        -0.14770
    111 ->124        -0.23791
    112 ->123         0.36075
    112 ->125        -0.10772
    113 ->123         0.22091
    113 ->125        -0.11068
    114 ->124         0.27721
    114 ->126         0.14405
```

```
     115 ->123         0.10903
     116 ->124        -0.10550
     118 ->127        -0.19283

 Excited State  68:      Singlet-A      6.1819 eV  200.56 nm  f=0.0035  <S**2>=0.000
     105 ->120        -0.17876
     109 ->123        -0.11395
     111 ->123        -0.20742
     112 ->124         0.31959
     113 ->124         0.23931
     113 ->126         0.16086
     114 ->123         0.21310
     114 ->125        -0.17777
     117 ->127         0.22412
     118 ->128         0.20052

 Excited State  69:      Singlet-B      6.1979 eV  200.04 nm  f=0.5873  <S**2>=0.000
     105 ->119        -0.21012
     106 ->120         0.32697
     109 ->122         0.11038
     113 ->123         0.15393
     115 ->123         0.12132
     116 ->124        -0.10507
     117 ->128         0.46978

 Excited State  70:      Singlet-A      6.2412 eV  198.66 nm  f=0.0101  <S**2>=0.000
     105 ->120         0.13466
     106 ->119        -0.23274
     113 ->124         0.47666
     114 ->123        -0.36842
     118 ->128         0.10904

 Excited State  71:      Singlet-B      6.2510 eV  198.34 nm  f=0.0294  <S**2>=0.000
     113 ->123         0.49929
     113 ->125        -0.12157
     114 ->124        -0.42905
     117 ->128        -0.11917

 Excited State  72:      Singlet-A      6.2594 eV  198.08 nm  f=0.0353  <S**2>=0.000
     104 ->120         0.15819
     105 ->120         0.17587
     106 ->119        -0.22434
     107 ->121        -0.14952
     108 ->122         0.14193
     113 ->124        -0.18329
     114 ->123         0.23893
     115 ->124         0.15246
     115 ->126         0.12414
     116 ->123        -0.16302
     117 ->127        -0.16690
     118 ->128         0.30143
 SavETr:  write IOETrn=   770 NScale= 10 NData=  16 NLR=1 NState=   72 LETran=
1306.
```

References

1 C.-Y. Chen, P.-Y. Cheng, H.-H. Wu and H.-M. Lee, *Inorg. Chem.*, 2007, **46**, 5691–5699.

2 (a) S. Zang, Y. Su, Y. Li, Z. Ni and Q. Meng, *Inorg. Chem.*, 2006, **45**, 174-180; (b) S. Zang, Y. Su, Y. Li, Z. Ni and Q. Meng, *Inorg. Chem.*, 2006, **45**, 2972-2978.

3 K. K. Bisht and E. Suresh, *J. Am. Chem. Soc.*, 2013, **135**, 15690-15693.

4 S.-H. Wang, F.-K. Zheng, M.-J. Zhang, Z.-F. Liu, J. Chen, Y. Xiao, A-Q. Wu, G.-C. Guo and J.-S. Huang, *Inorg. Chem.*, 2013, **52**, 10096–10104.

5 M. R. Bermejo, M. Vázquez, J. Sanmartín, A. M. García-Deibe, M. Fondo and C. Lodeiro, *New J. Chem.*, 2002, **26**, 1365-1370.

6 V. Balamurugan and R. Mukherjee, *CrystEngComm*, 2005, **7**, 337–341.

7 (a) U. Siemeling, I. Scheppelmann, B. Neumann, A. Stammler, H. -G. Stammler and J. Frelek, *Chem. Commun.*, 2003, 2236–2237; (b) J. Breu, H. Domel and A. Stoll, *Eur. J. Inorg. Chem.*, 2000, 2401–2408 and references cited therein.

8 (a) M. Enamullah, M. A. Quddus, M. R. Hasan, G. Pescitelli, R. Berardozzi, G. Makhloufi, V. Vasylyeva and C. Janiak*, Dalton Trans.*, 2016, **45**, 667−680; (b) M. Enamullah, M. A. Islam, B. A. Joy and G. J. Reiss, *Inorg. Chim. Acta*, 2016, **453***,* 202−209.

9 (a) M. Enamullah, G. Makhloufi, R. Ahmed, B. A. Joy, M. A. Islam, D. Padula, H. Hunter, G. Pescitelli and C. Janiak, *Inorg. Chem.*, 2016, **55**, 6449−6464; (b) M. Enamullah, M. A. Quddus, M.A. Halim, M. K. Islam, V. Vasylyeva and C. Janiak, *Inorg. Chim. Acta*, 2015, **427***,* 103−111.

10 Mercury CSD 3.9, program for crystal structure visualisation, exploration and analysis from the Cambridge Crystallographic Data Center, Copyright CCDC 2001-2016, http://www.ccdc.cam.ac.uk/mercury/

12 K. Brandenburg, Diamond (Version 3.2), Crystal and Molecular Structure Visualization, Crystal Impact – K. Brandenburg & H. Putz Gbr, Bonn (Germany) **2009**.

12 (a) M. Nishio, *Phys. Chem. Chem. Phys.*, 2011, **13**, 13873-13900; (b) M. Nishio, Y. Umezawa, K. Honda, S. Tsuboyama and H. Suezawa, *CrystEngComm*, 2009, **11**, 1757-1788; (c) M. Nishio, *CrystEngComm*, 2004, **6**, 130-158; (d) C. Janiak, S. Temizdemir, S. Dechert, W. Deck, F. Girgsdies, J. Heinze, M. J. Kolm, T. G. Scharmann and O. M. Zipffel, *Eur. J. Inorg. Chem.*, 2000, 1229-1241; (e) Y. Umezawa, S. Tsuboyama, K. Honda, J. Uzawa and M. Nishio, *Bull. Chem. Soc. Jpn.*, 1998, **71**, 1207-1213.